Velocity Fluctuation and Cellular Structure of Near-Limit Detonations in Rough Tubes

Tianfei Ren[1,2], Yiran Yan[3,4], John H.S. Lee[2†], Hoi Dick Ng[5], Qingming Zhang[1†] and Cheng Shang[1]

[1] State key Laboratory of Explosion Science and Technology, Beijing Institute of Technology, Beijing 100081, China

[2] Department of Mechanical Engineering, McGill University, Montreal, QC, H3A 0C3, Canada

[3] Global energy Internet Research Institute Co., Ltd, Beijing 102209, China

[4] State Grid Key Laboratory of Information & Network Security，Beijing 102209, China

[5] Department of Mechanical, Industrial and Aerospace Engineering, Concordia University, Montreal, QC, H3G 1M8, Canada

[†]Corresponding Author

State key Laboratory of Explosion Science and Technology
Beijing Institute of Technology
Beijing 100081, China
E-mail: qmzhang@bit.edu.cn

Department of Mechanical Engineering
McGill University
Montreal, QC, H3A 0C3, Canada
E-mail: john.lee@mcgill.ca

Revised manuscript submitted to *Fuel*

November, 2020

Velocity Fluctuation and Cellular Structure of Near-Limit Detonations in Rough Tubes

Tianfei Ren[1,2], Yiran Yan[3,4], John H.S. Lee[2†], Hoi Dick Ng[5], Qingming Zhang[1†] and Cheng Shang[1]

[1] State key Laboratory of Explosion Science and Technology, Beijing Institute of Technology, Beijing 100081, China

[2] Department of Mechanical Engineering, McGill University, Montreal, QC, H3A 0C3, Canada

[3] Global energy Internet Research Institute Co., Ltd, Beijing 102209, China

[4] State Grid Key Laboratory of Information & Network Security, Beijing 102209, China

[5] Department of Mechanical, Industrial and Aerospace Engineering, Concordia University, Montreal, QC, H3G 1M8, Canada

Abstract

Detonation limits are characterized by a decrease in the propagation velocity, cellular structures to lower unstable modes and an increase in the velocity fluctuation of the detonation. The increase in the average velocity deficit as the limits are approached is not a sensitive change since the failure of the detonation can occur at a relatively small velocity deficit of the order of 20%. A more sensitive indication of the onset of detonation limits is the lowering of the unstable mode (i.e., towards single-headed spin) and the large longitudinal fluctuation of the detonation velocity. In this paper, recent results are reported for the aforementioned near-limit detonation characteristics for a number of detonable mixtures and tube diameters for both smooth and rough tubes. Mixtures include H_2, C_2H_2, C_3H_8, CH_4 fuels with both O_2 or N_2O as oxidizers. Tube diameters were 25.4 mm, 38.1 mm, 50.8 mm and 76.2 mm. To investigate the effect of wall roughness on the limits phenomena in tubes, wire spirals with different diameters were inserted into the different diameter test tubes. Regularly spaced photodiodes (IF-950C) along the tube were used for velocity measurements and smoked mylar foils were inserted into the tube for the measurement of the cellular structure. Results confirm that the cellular structure evolution towards the lower unstable modes follows well the observed increase in velocity fluctuation; the subsequent detonation failure defined by the absence of cells occurs also at high-velocity fluctuation and an abrupt increase in the average velocity deficit.

Keywords: Detonation limits; Wall roughness; Velocity deficits; Velocity fluctuation; Smoked foils; Cellular Structure

1 Introduction

Near-limit behavior of detonation has been studied especially in recent years due to increasing interests in the detonation-based propulsion concept, e.g., [1-3]. Detonation limits are defined as the conditions outside of which self-sustained propagation of detonation wave is not possible [4]. In general, detonation limits can be brought about by too lean or too rich a mixture composition and an increase in the concentration of an inert diluent. At these limiting fuel-air equivalence ratios and dilutions, the performance of an air-breathing detonation-based engine such as pulse detonation engine PDE can be significantly affected by the near-limit behavior of detonation. Alternatively, detonation limits could also be reached and investigated by the decrease in initial pressure for a mixture of a given composition or the change of boundary conditions in a given geometry, e.g., near-limit behavior of detonations in narrow channels of rotating detonation engines RDEs and PDE pre-detonator tubes. Fundamentally, limits phenomena provide a good setting as well to investigate the failure and propagation mechanism of detonation waves [4].

Substantial studies have been carried in recent decades to investigate the steady velocity deficits near the limits, e.g., [5-15]. In addition, a spectrum of instability phenomena near limits have been revealed by a number of investigations [16-27]. Despite extensive studies on detonation limits, the failure mechanism remains obscure. In fact, to explore in detail the near-limit detonation propagation behavior and subsequently the failure, one must investigate the instability of the front as the limits are approached. This study is put forward a good way to describe the near-limit behavior of detonation waves.

Generally speaking, when the limits occur, the detonation velocity fluctuation increases and the unstable cellular structure is driven to lower unstable modes, i.e., from multi-headed to single-headed spinning detonations. It is also observed that either for smooth or rough tubes, the fluctuation of the detonation velocity is rather small far away from the limits but increases as the initial pressure is reduced towards the limits. It thus appears that the velocity fluctuation would be an interesting measure of the ability for self-sustained propagation of the detonation in both smooth and rough tubes.

Another crucial phenomenon in photographic observations can be obtained by smoked foils. Smoked foils could be inserted from the end of the test tube to register the cellular detonation structure near or well within the detonation limits. Smoked foil diagnostics could indicate that the detonation structure goes towards lower unstable mode: from multi-headed to single-headed at the limits. Since single-headed spinning detonation corresponds to the limiting structure of a self-sustained detonation, any absence of cellular feature at the detonation front could provide a better indication of the detonation failure.

In the present paper, extensive information on both the velocity fluctuation and cellular structure as the detonation limits are approached in both smooth and rough walled tubes are reported. In contrast to many previous studies using repeated orifice plate obstacles [28-36] where the dimensions of the orifice diameter and spacing are of the order of the tube diameter itself, the wall roughness was introduced here by using different spiral inserts whose dimension is small as compared to the tube diameter. In this way, unlike in orifice plates-filled tubes where the diffraction of the detonation through the orifice and reflections from the orifice plate and the tube wall of the diffracted front play major roles in the failure and ignition as the detonation propagates past the obstacles, the effect of the wall roughness generated by small helical spirals creates only small perturbations on the detonation and the flow field associated with the detonation front. The use of rough walled tubes is motivated by recent studies showing the wall roughness has a strong influence either on the propagation velocity fluctuation and the cellular structure of the detonation wave near the limits [37-43]. A variety of explosive mixtures with different detonation sensitivity, tube diameter as well as spiral geometric parameters in rough walled tubes were considered.

2 Experimental Details

Figure 1 describes the experimental apparatus used in this study. It consists of two sections: driver and test sections. The driver section has a diameter D = 25.4 mm, and the test section has either D = 25.4 mm, 38.1 mm, 50.8 mm, or 76.2 mm. A Shchelkin spiral was inserted in the driver section to promote the initial detonation formation. A variety of pre-mixed mixtures, i.e., $H_2 + N_2O$, $C_2H_2 + 5N_2O$, $C_2H_2 + 2.5O_2$, $C_3H_8 + 5O_2$, $2H_2 + O_2$ and $CH_4 + 2O_2$ were tested. Gaseous detonation dynamics, including initiation and propagation limits, are known to be affected by the inherent instability of the detonation structure. The mixtures tested in this work are commonly used in laboratory-scale studies and considered in the literature. These non-diluted mixtures are typically referred to as unstable mixtures, in which the cellular detonation structures are irregular. The use of these different fuels and oxidizers provides some variation in the detonation instability (or slight difference of cellular pattern irregularity) and allows us to observe if there is any hidden effect of the chemistry on the near-limit behavior of detonation. The sensitivity of these mixtures is varied by changing the initial pressure in the range from 0.5 kPa to 30 kPa.

To generate wall roughness, 1.5-m long spirals with a wire diameter of 1 mm, 2 mm, 3 mm were used for the 25.4-mm-diameter tube; 1.5 mm, 3 mm, 5 mm, 6.5 mm for the 38.1-mm-diameter tube, 1.5 mm, 3 mm, 6.2 mm and 9 mm for the 50.8-mm-diameter tube; and finally, 9 mm and 11 mm for the 76.2-mm-diameter tube. In all cases, the pitch of the spring is double the wire diameter of each spring. Figure 1(b) provides further details on all the spirals used in the experiments and the tested mixtures in different tube sizes are summarized in Table 1. In few cases, e.g., for the less sensitive mixtures such as $2H_2 + O_2$ or mixtures at very low initial pressure, a small amount of more sensitive $C_2H_2 + O_2$ mixture was injected into the driver section for the detonation initiation. Optical fibers terminating at a photodiode (IF-950C) were spaced at regular intervals along the tube for velocity measurements. From the time-of-arrival data, the detonation trajectory is obtained from which the propagation velocity can be determined. Standard smoked foil technique using soot mylar foils inserted into the tube was employed to observe the evolution of the detonation cellular structure. At least three repeated experiments at the same condition were carried out to ensure the repeatability of the measurement results.

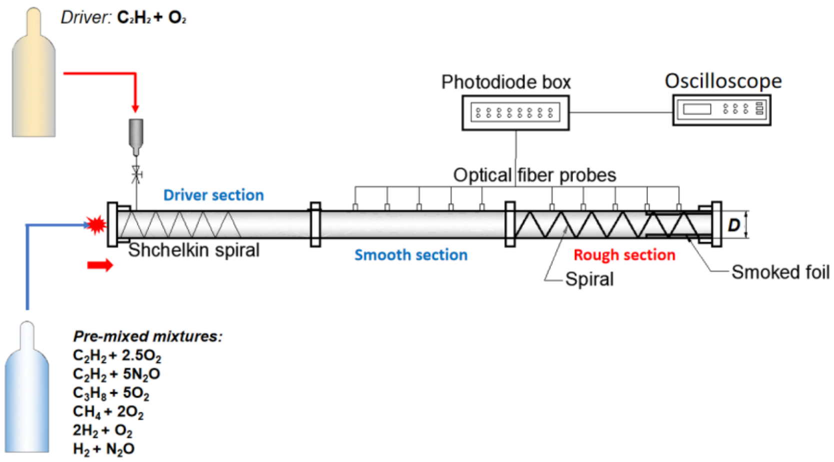

(a)

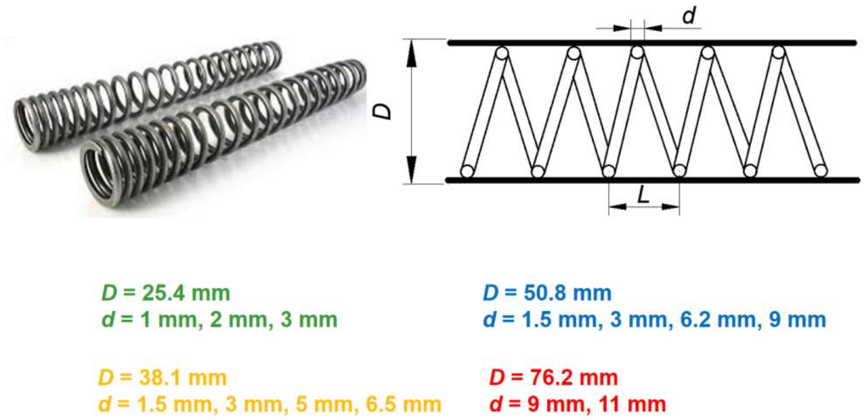

(b)

Figure 1. Sketch of the experimental apparatus (a) and spiral parameters (b) [42]

Table 1 The experimental conditions

Tube diameter / Mixture	25.4 mm	38.1 mm	50.8 mm	76.2 mm
C_2H_2+2.5O_2	✓	✓	✓	✓
C_2H_2+5N_2O		✓	✓	

CH_4+2O_2		✓	✓	
C_3H_8+5O_2		✓		
2H_2+O_2		✓	✓	
H_2+N_2O	✓	✓	✓	✓

2 Results and Discussion

From Fay's [44] theory, a theoretical model could be formulated to predict the velocity deficit of the detonation wave while approaching the limits in small tubes, see Eq. (1).

$$\frac{\Delta V}{V_{\mathrm{CJ}}} = \frac{V_{\mathrm{CJ}} - \upsilon}{V_{\mathrm{CJ}}} \tag{1}$$

It is a classical analysis based on the flow divergence to estimate the velocity deficit. In detail, the velocity deficit is due to the boundary layer growth on the tube wall producing a uniform flow divergence throughout the detonation front. From the quasi-steady Zel'dovich-von Neumann-Döring (ZND) model, this flow divergence causes less energy to be released in the reaction zone before the sonic state is attained, under-driving the detonation wave and causing wave propagation at a decreased velocity. The model is well described in the original paper by Fay [44] and many other recent papers on detonation limits, e.g., [45, 46], as well as in Lee's monograph on the detonation phenomenon [4]. In short, based on the one-dimensional ZND structure, Eq. (1) can be written as follows:

$$\frac{\Delta V}{V_{\mathrm{CJ}}} = 1 - \left[\frac{(1-\upsilon)^2}{(1-\upsilon)^2 + \gamma_1^2(2\nu - \nu^2)}\right] \tag{2}$$

ΔV is the detonation velocity deficit, V_{CJ} is the theoretical Chapman-Jouguet CJ detonation velocity, υ is the actual detonation velocity. γ_1 denotes the specific heat ratio of a given mixture obtained from thermodynamic calculation. The actual velocity can also be related by:

$$\nu = \frac{\varepsilon}{(1+\gamma_1)(1+\varepsilon)} \tag{3}$$

where ε represents the area divergence. It is determined by the boundary layer displacement thickness δ* and the inner diameter D of the circular tube as follows:

$$\varepsilon = \frac{A_1}{A_0} - 1 = \frac{\pi\left(\frac{D}{2}+\delta^*\right)^2}{\pi\left(\frac{D}{2}\right)^2} - 1 \approx \frac{4\delta^*}{D} \tag{4}$$

$$\delta^* = 0.22 l^{0.8} \left(\frac{\mu_{\mathrm{e}}}{\rho_0 V_0}\right)^{0.2} \tag{5}$$

where l refers to the reaction zone thickness (in mm). and μ_e (in Pa·s), V_0 (in m/s), and ρ_0 (in kg·m^{-3}) represent the viscosity, detonation velocity, and initial density of the pre-reaction mixture, respectively. To estimate the reaction zone thickness, l, Lee [4] suggested that it can be considered to be roughly equal to the detonation cell length. The latter can be correlated with the ZND induction zone length using an empirical formula. Another approach is also proposed by Zhang [46], on the basis of the work of Crane et al. [47] for the reaction zone thickness approximation, including both the induction zone length (Δ_I) and the exothermic length (Δ_R). For simplicity, we use Lee's method for approximating l and the cell size is estimated using the linear relationship with the steady ZND induction length obtained from the CHEMKIN-II package [48].

Here, results from Fay's model are compared with the present experimental data as a cross-check. As an example, Fig. 2 shows the normalized velocity of CH_4 + $2O_2$ in roughness tubes with diameters D = 50.8 mm obtained from the experiment and theoretical prediction. The maximum difference is found to be under 15%. This comparison provides indirectly a level of credibility of the experimental data.

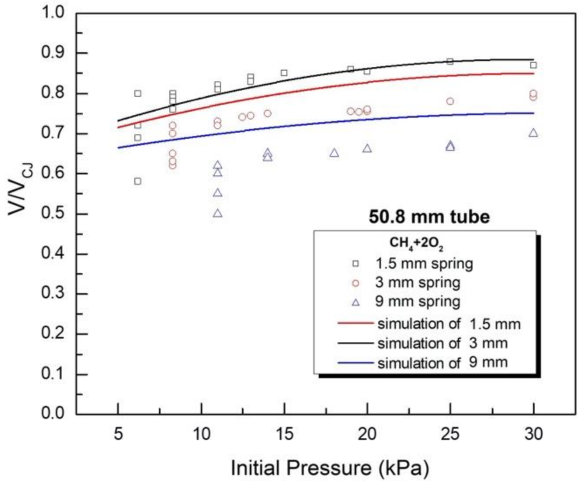

Figure 2. Comparison of the normalized velocity of $CH_4 + 2O_2$ between experiments and theoretical prediction in the D = 50.8 mm tube.

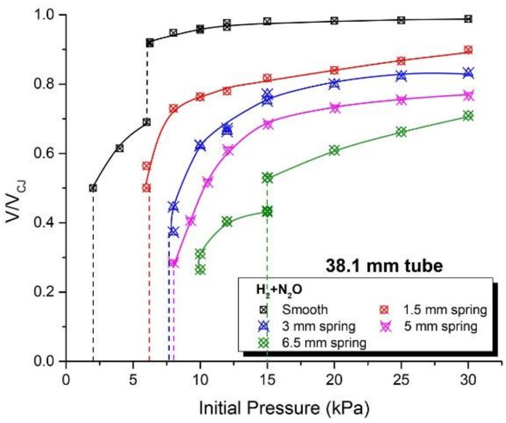

(a)

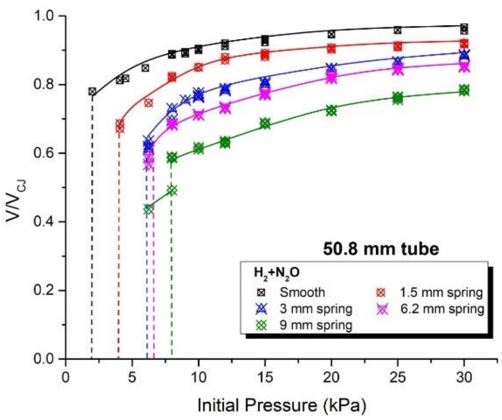

(b)

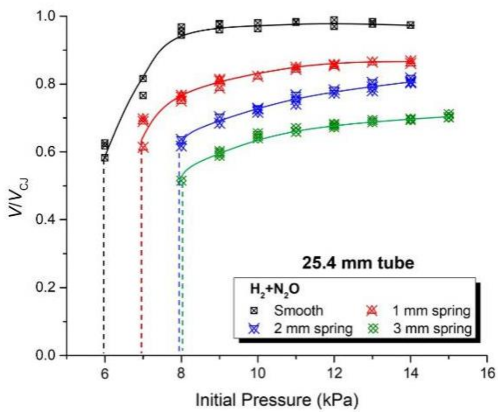

(c)

Figure 3. The normalized velocity of H_2 + N_2O in both smooth and roughness tubes with different diameters *D*.

Sample results for the variation of the average detonation velocity with decreasing initial pressures gradually towards the limits are shown in Fig. 3 for H_2 + N_2O in both smooth and rough tubes with either 25.4 mm, 38.1 mm, or 50.8 mm diameter. The average velocity was determined from the slope of the wave trajectory in the *x*-*t* plots using the time-of-arrival measurement by the photodiodes [42]. At least three shots (and particularly more near the limiting pressure) were performed for each condition to ensure the reproducibility of the results. Again, for a smooth tube, far from the limits, the normalized velocity is close to the CJ value and thus, the velocity deficits are small. As the initial pressure decreases towards the limits the detonation velocity decreases progressively until the onset of the limits where the velocity drops abruptly. The abrupt velocity drop indicates that a robust detonation propagating at a steady high velocity cannot be sustained and the rapid decoupling of the leading shock front with the reaction zone causes the wave to decay and fail. The minimum average velocity seldom drops below 80% of the CJ value. Meanwhile, a generally similar phenomenon was recorded in the rough tubes as the limits are approached. However, for rough walled tubes, the velocity deficit increases with increasing roughness (generated by larger wire diameter spirals). The limits defined by the velocity drop also occur at higher initial pressure with increasing roughness. This indicates that the roughness in turn narrows the detonation limits. In some conditions, past the limits, the wave could decay to a deflagration with a relatively low average velocity as small as 0.40 V_{CJ}. A second velocity drop occurs when these high-speed deflagration waves cannot be sustained or fail. As discussed in [42], these low-velocity combustion waves cannot be considered as a detonation due to the absence of cellular structures irrespective of its velocity.

Following Manson et al. [49], the velocity fluctuation is defined as $\delta = |V_l - V_m|/V_m$ where V_l is the local detonation velocity and V_m is the average velocity over the length of propagation of the detonation along the tube. In the present study, the velocity fluctuation of the leading wave front from the velocity measurement using the photo-probes is also determined. Although not all the compression waves or flow structure behind the front are measured, the velocity fluctuations of the propagating wave front can still provide a good description of the near-limit propagation behavior of the detonation and onset of limits. The velocity fluctuation δ describes at least the first-order behavior of the detonation when it approaches the limits. As argued in Manson et al. [49], the increase in the wave front velocity fluctuation provides some instability parameter indicating the loss of robustness of the cellular detonation when it approaches the limit. Hence, there is merit to look at the fluctuating nature of the propagating front despite the fact that a range of pressure waves activities may be present behind it.

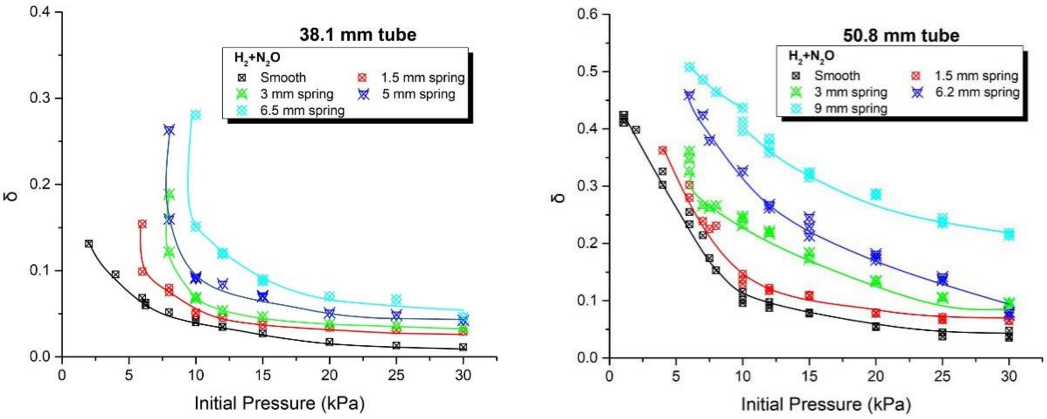

(a) **(b)**

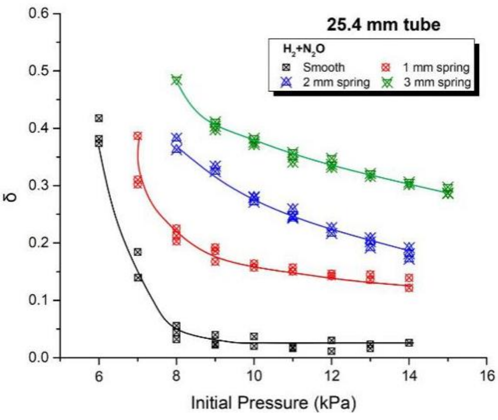

(c)

Figure 4 The velocity fluctuation of detonation of H_2 + N_2O in both smooth and roughness tubes with different diameters *D*.

With the increase of the roughness as the initial pressure decreases, the fluctuation of the detonation velocity δ shows an increase, and the local value of detonation velocity can be as low as about 0.4 V_{CJ} near the limit, no matter what the tube diameter is. Figure 4 shows the variations of the maximum velocity fluctuation δ for the mixtures H_2 + N_2O with initial pressures, which correspond to the results of Fig. 3. It can be observed that the velocity fluctuation is small far from the limits but increases rapidly as the limits are approached, as higher as about 0.4. This indicates that the longitudinal propagation of the detonation is very unstable as the limits are approached.

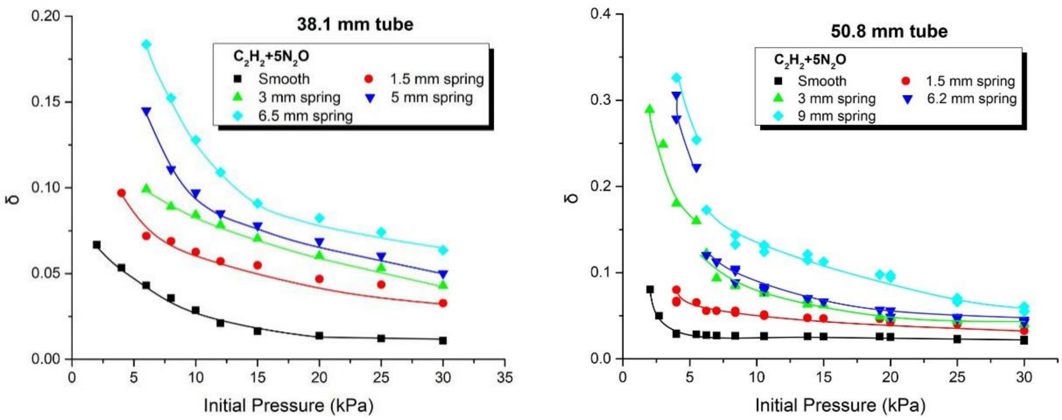

(a) **(b)**

Figure 5 The velocity fluctuation of detonation of C_2H_2 + $5N_2O$ in both smooth and roughness tubes with different diameters *D*.

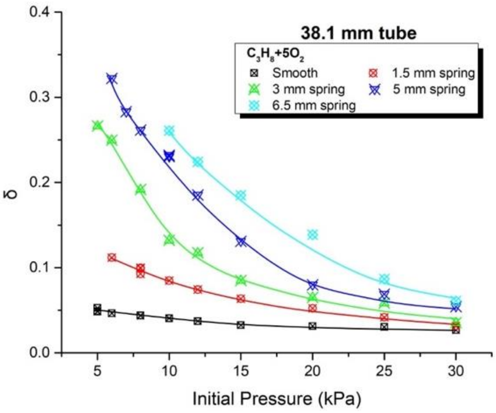

Figure 6 The velocity fluctuation of detonation of C_3H_8 + $5O_2$ in both smooth and roughness tubes with *D*= 38.1 mm.

Similarly, Figs. 5 and 6 display velocity fluctuation results for the mixtures of C_2H_2 + $5N_2O$ and C_3H_8 + $5O_2$, respectively. Again, for these two mixtures, at high initial pressure far from the limits only small velocity fluctuation (possibly due to the intrinsic instability and the presence of wall roughness) were recorded regardless of smooth or rough walled tubes. As the initial pressure gradually reduces to approach the limits, the velocity fluctuation rises again rapidly and the fluctuation value also increases with increasing roughness. For conditions typically with a high level of wall roughness, where a high-speed deflagration is sustained past the detonation limits, a second branch with even higher δ can be seen, see Fig. 5 (b).

By analyzing the smoked foils records, the evolution of cellular detonations can be observed as limits are approached. When the initial pressure is reduced towards the limits, it is well observed that the cellular detonation structures can be seen to decrease to the lower unstable mode in both the smooth and the rough tubes. The detonation failure can be signified by the absence of any cellular detonation structure. Our recent study also confirms that the disappearance of cellular detonation pattern corresponds also the significant increase of velocity deficit as shown in Fig. 3 [42]. All results indicate that when the wall roughness of the tube is considered, the detonation wave is affected significantly to various degrees. Therefore, the influence of wall roughness is mainly analyzed below. Figure 7 shows some smoked foils results for $2H_2 + O_2$ detonation propagation under the effect of wall roughness. As tube wall roughness increases, the cellular structure evolves towards the lowest unstable mode, i.e., single head spin, at higher initial pressure. In other words, again, wall roughness tends to narrow the detonation limits. Generally, the roughness induces losses resulting in the velocity deficit and creates perturbation on the detonation flow field. When the conditions are far from the limits, the intrinsic unstable cellular structure of the detonation is quite robust and retains its global dynamic characteristics. However, when the limits are approached, the unstable mode changes toward the lowest fundamental mode and begins to lose its robustness, becoming more sensitive to perturbations. Hence, due to the additional losses and flow perturbations, the roughness tends to drive the detonation to lower unstable modes and to fail earlier at higher critical pressure.

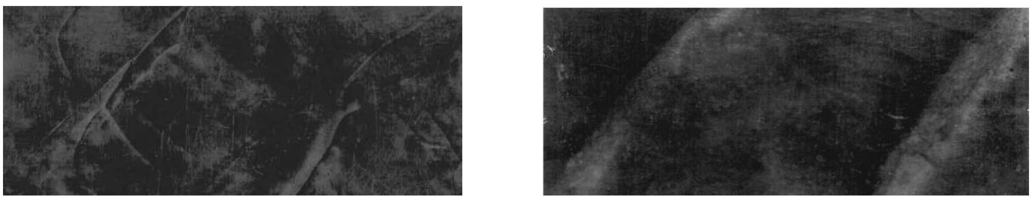

P_0 = 8 kPa, 1.5 mm spring P_0 = 9.8 kPa, 3 mm spring

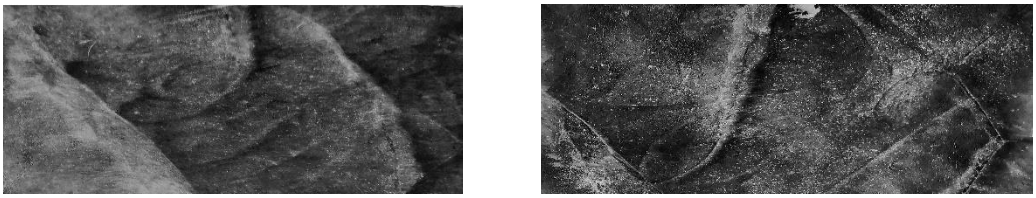

P_0 = 11 kPa, 6.2 mm spring P_0 = 14 kPa, 9 mm spring

Figure 7 Single-headed cellular structures of $2H_2 + O_2$ in the D = 50.8 mm rough tube

Next, it is of interest to directly compare also the cellular structure obtained from the smoked foils results with the fluctuation of the detonation velocity δ. Figure 8 shows from the soot foils the cellular detonation structures for $C_2H_2 + 2.5O_2$ in the 25.4-mm-diameter and 76.2-mm-diameter smooth and rough tubes that could manifest as the initial pressure is reduced towards the corresponding limits.

In Fig. 8(a) showing the results for the 25.4-mm-diameter tube, the four points (**i** to **iv**) on the velocity fluctuation plot indicates the different initial pressure values where the smoked foils are simultaneously obtained in the smooth tube. These correspond to: **i)** P_0 = 3 kPa where a multi-headed cellular detonation is observed with relatively small velocity fluctuation δ = 0.18; **ii)** P_0 = 1.5 kPa, at which a multi-headed cellular structure is still maintained but with larger cell size, and the detonation fluctuation increases to δ = 0.21; **iii)** P_0 = 0.7 kPa where the single-headed spin structure is attained and the detonation approaches the limit with a large fluctuation δ = 0.45; and finally, **iv)** P_0 = 0.5 kPa, the detonation fails and the cellular structure vanishes completely with the value of velocity fluctuation increased to δ = 0.5. Equivalently, four smoked foils obtained from the experiments with a 3 mm spring introduced in the tube, as a simulation of a rough wall, are also shown in Fig. 8(a). The initial pressures for these smoked foils are labeled (**1**) to (**4**). Similar cellular structure evolution and velocity fluctuation trend can be seen, but carried out at higher initial pressures.

Similarly, in Fig. 8 (b) showing the results for the $C_2H_2 + 2.5O_2$ in the 76.2-mm-diameter tube, the selected initial pressure values for each smoked foil in smooth tubes are: **i)** $P_0 = 4$ kPa, **ii)** $P_0 = 1.5$ kPa; **iii)** $P_0 = 0.7$ kPa; and **iv)** $P_0 = 0.5$ kPa. In this decreasing order of initial pressure, the cellular pattern changes from the multi-headed structure (**i**, **ii**) to single-head spin (**iii**) and then failure (**iv**), respectively. The velocity fluctuation before failure increases again to approximately $\delta \sim 0.5$. For the rough tube case with a 11 mm spring, the initial pressure points are: **1**) $P_0 = 3$ kPa; **2**) $P_0 = 1.2$ kPa; and **3**) $P_0 = 1$ kPa. All trends are similar to the smooth tube result but the limit conditions come up to higher initial pressure and also the detonation is driven to the lowest unstable mode at a higher initial pressure value.

In short, Fig. 8 demonstrates notably that the cellular detonation structure goes towards lower unstable modes in both smooth and rough tubes. The cellular pattern evolution follows well the velocity fluctuation trend, where the cellular detonation changes from multi-headed to single-head spin, and eventually to failure devoid of cellular structures occurs at increasing δ. Either the change of roughness or the diameter of the tube will effect the same change of cellular structure toward low modes: from multi-headed to single-headed.

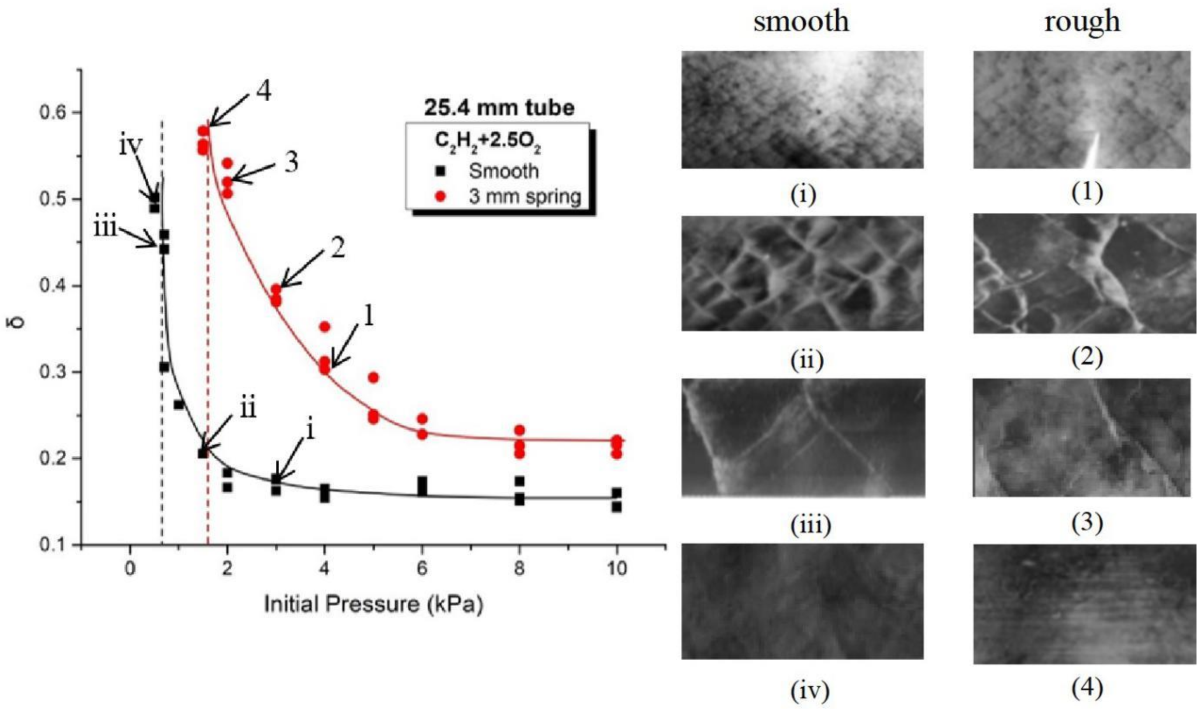

(a)

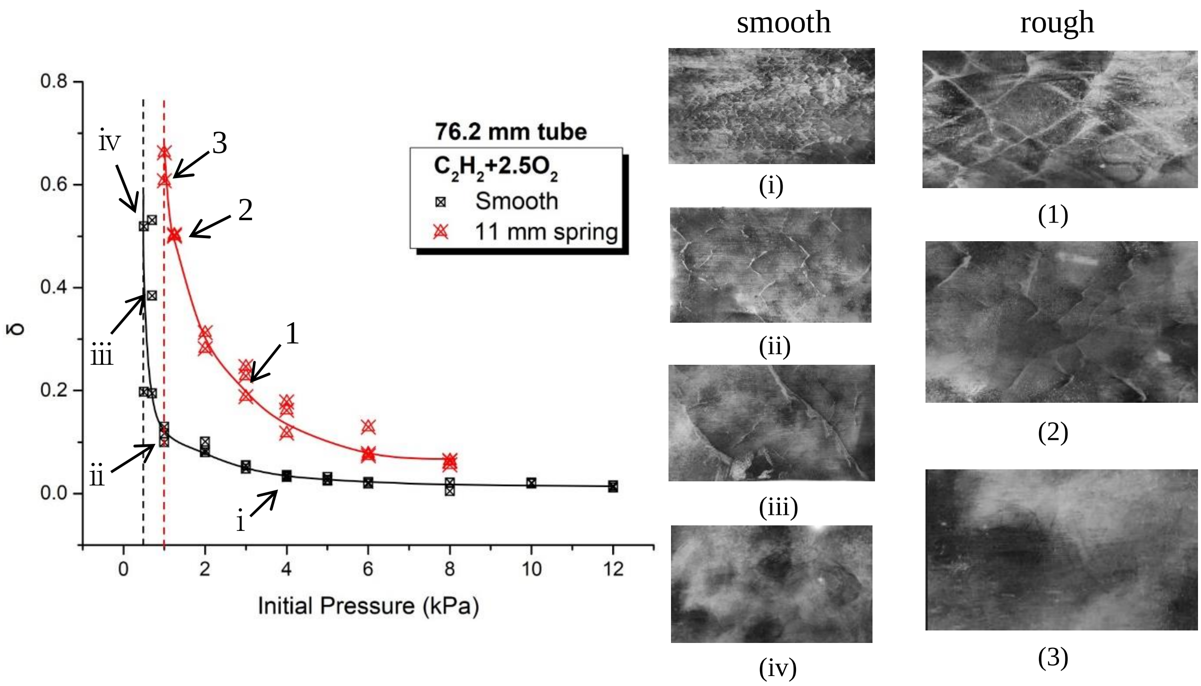

(b)

Figure 8 Smoked foils and the velocity fluctuation for C_2H_2 + $2.5O_2$ with the smooth tube and the rough tube in (a) 25.4-mm-diameter; and (b) 76.2-mm-diameter.

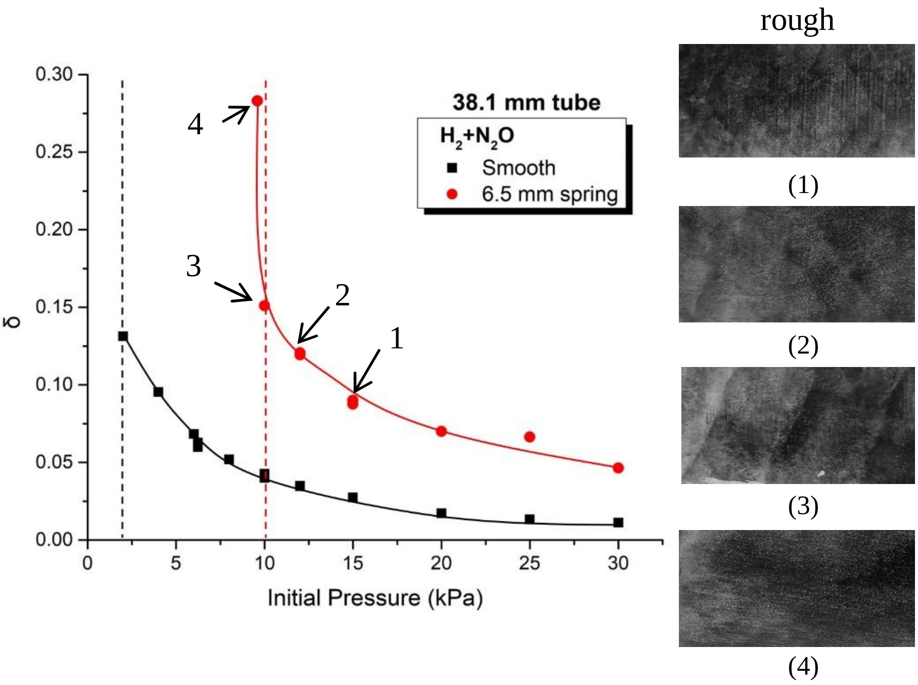
rough
(1)
(2)
(3)
(4)
38.1 mm tube
H2+N2O
Smooth
6.5 mm spring
δ
Initial Pressure (kPa)
0.00
0.05
0.10
0.15
0.20
0.25
0.30
0
5
10
15
20
25
30
1
2
3
4

(a)

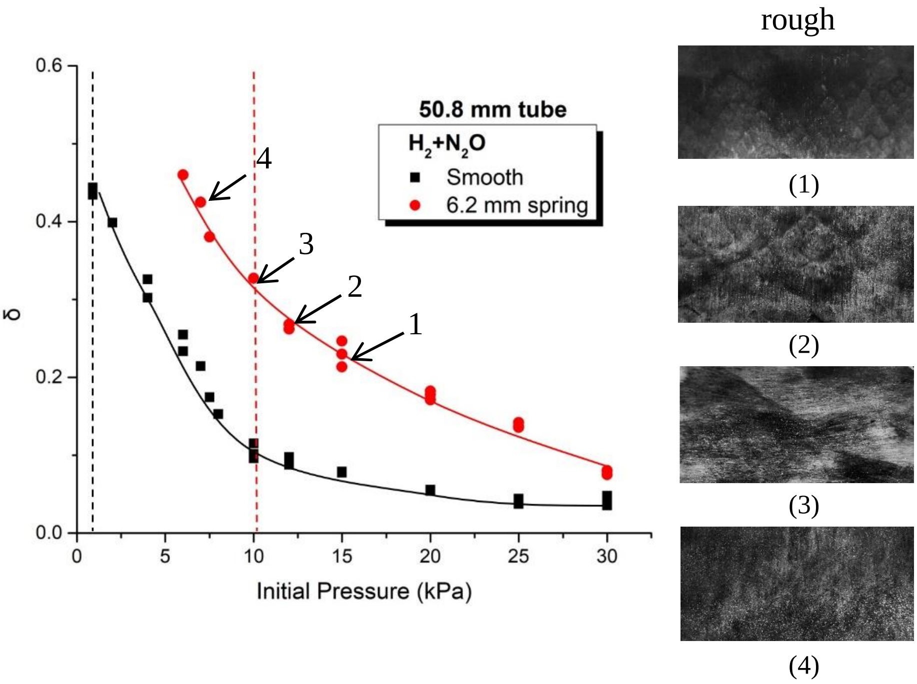
rough
(1)
(2)
(3)
(4)
50.8 mm tube
H2+N2O
Smooth
6.2 mm spring
δ
Initial Pressure (kPa)
0.0
0.2
0.4
0.6
0
5
10
15
20
25
30
1
2
3
4

(b)

Figure 9 Smoked foils and the velocity fluctuation for H_2 + N_2O with the rough tube in (a) 38.1-mm-diameter; and (b) 50.8-mm-diameter.

For completeness, additional smoked foils records of the different mixtures H_2 + N_2O, C_2H_2 + $5N_2O$ and C_3H_8 + $5O_2$ are provided together with the corresponding velocity fluctuation curves in Figs. 9 to 11. Again, comparing the results between the smooth and rough walled tubes shows that the abrupt increase in velocity fluctuation occurs at higher limiting initial pressure for increasing tube wall roughness. Similar to Fig. 8, the single head spin and subsequently the detonation failure follows the increasing trend in the velocity fluctuation.

To summarize, for the H_2 + N_2O results with D = 38.1 mm shown in Fig. 9 (a), the four points correspond to the initial pressure **1**) P_0 = 15 kPa; **2**) P_0 = 12 kPa; **3**) P_0 = 10 kPa; and **4**) P_0 = 9.8 kPa, respectively. The single head spin would come at P_0 = 10 kPa. In Fig. 9 (b), the tube diameter increases to D = 38.1 mm and four points of initial pressure are **1**) P_0= 15 kPa; **2**) P_0 = 12 kPa; **3**) P_0 = 10.56 kPa; and **4**) P_0 = 7 kPa. The single head spin would come at P_0 = 10.56 kPa which is just a little higher than the result for D = 38.1 mm. For the mixture of C_2H_2 + $5N_2O$, Fig. 10 (a) shows that the smoked foils at the initial pressure **1**) P_0 = 10 kPa; **2**) P_0 = 8 kPa; **3**) P_0 = 7 kPa; and **4**) P_0 = 6 kPa, and the single head spin would come at **3**) P_0 = 7 kPa. Figure 10 (b) shows that the initial pressure **1**) P_0 = 8 kPa; **2**) P_0 = 7 kPa; **3**) P_0 = 5.5 kPa; **4**) P_0 = 4 kPa, and the single head spin would come at P_0 = 5.5 kPa. For **4**) P_0 = 4 kPa, the high velocity fluctuation δ branch corresponds to the high-speed turbulent deflagration discussed previously and the smoked foil indicates no cellular structure.

For each of the above mixtures, considering the relatively small variation in the initial pressure for the onset of single-head spin for the two diameters D = 38.1 mm and 50.8 mm while the roughness parameters kept almost the same, it shows that the detonation structure is primarily influenced by the roughness. For Fig. 11, the mixture of $C_3H_8 + 5O_2$ for tube diameter D = 38.1 mm, the single head spin would come at P_0 = 10 kPa.

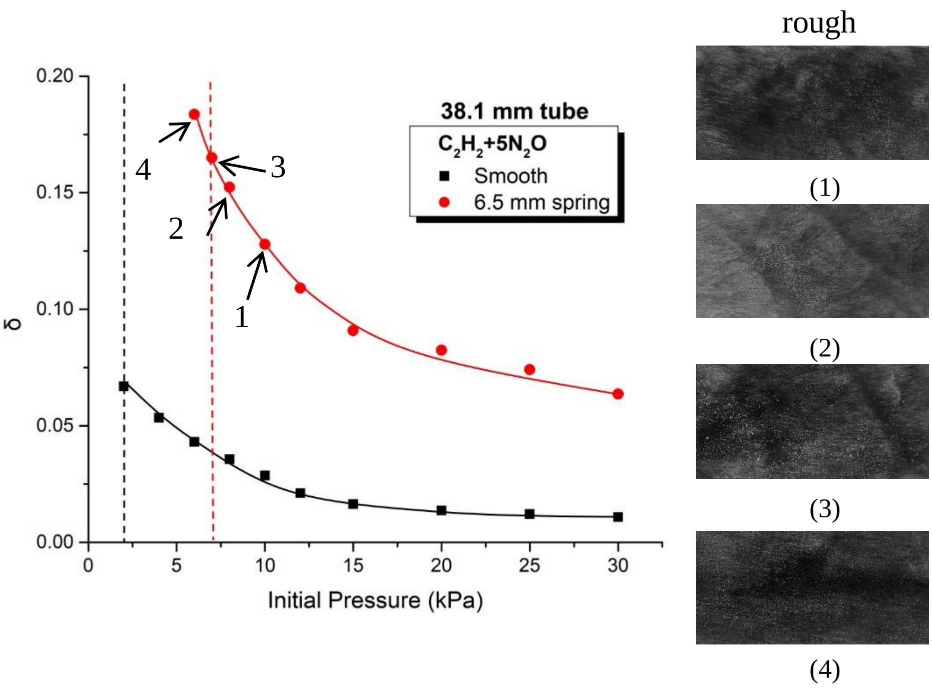

(a)

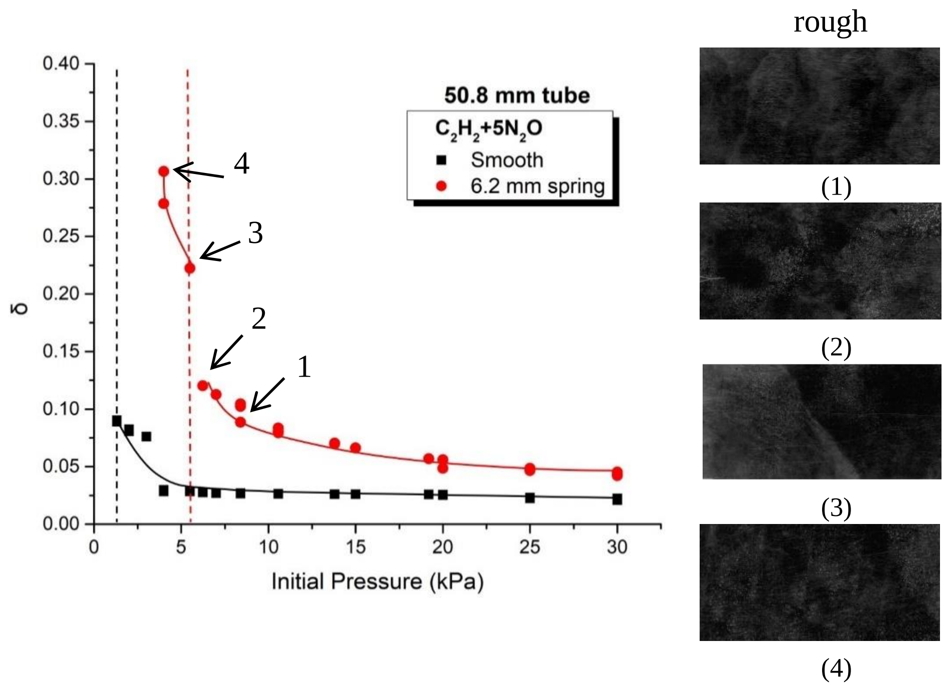

(b)

Figure 10 Smoked foils and the velocity fluctuation for C_2H_2 + $5N_2O$ with the rough tube in (a) 38.1-mm-diameter; and (b) 50.8-mm-diameter.

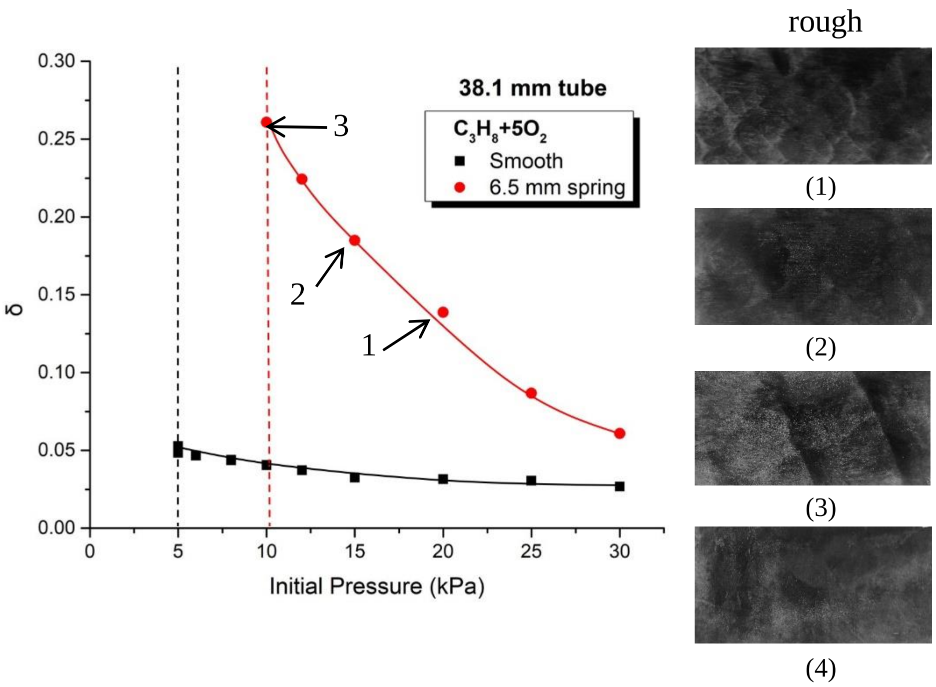

Figure 11 Smoked foils and the velocity fluctuation for C_3H_8 + $5O_2$ with the *D* = 38.1-mm-diameter rough tube. (*Note: (iv) corresponds to a failure case where no signal was registered by the photoprobes.)*

Figure 12 shows the results obtained of the CH_4 + $2O_2$ mixture with tube diameter *D* = 38.1 mm and different degrees of wall roughness at the same initial pressure. At P_0 = 15 kPa and the spring coil equal to 3 mm, the detonation structure has 4 - headed spins spin structure, but when the spring coil wire diameter is increased to 6.5 mm, a single-headed structure is indicated. It indicates that at the same initial pressure condition, the large spring coil wire diameter, i.e., a higher degree of roughness, may cause more losses and perturbations, resulting in the cellular structure to approach lower unstable mode at a higher initial pressure.

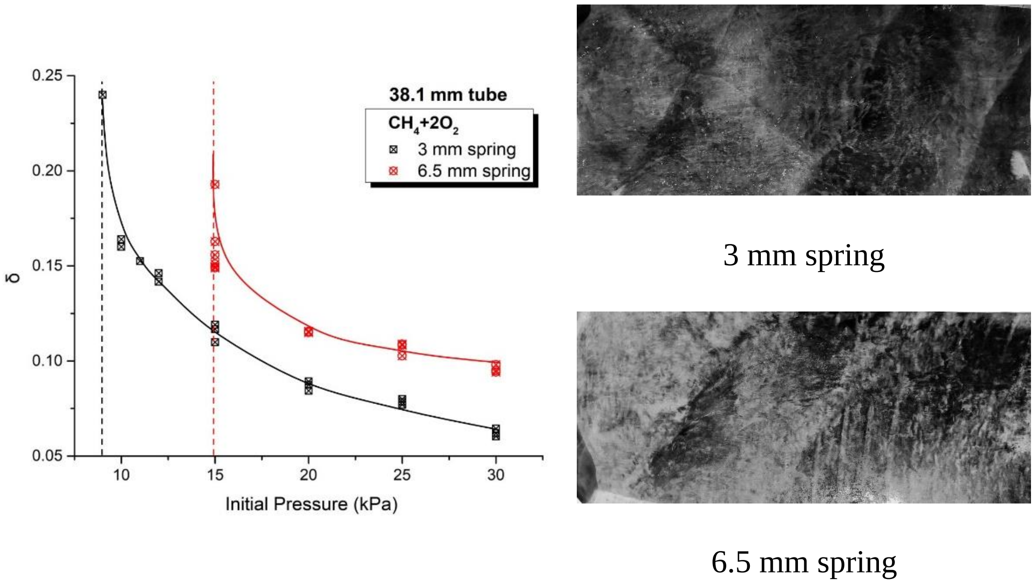

Figure 12 The cellular structures at the same initial pressure for $CH_4 + 2O_2$ in two different rough tubes.

5 Conclusions

In this study, the effect on velocity fluctuation and detonation structure by the rough wall was investigated. The experimental results are verified with Fay's model for the velocity deficits. The detonation structure is shown to play a prominent role in the detonation limits. The longitudinal velocity fluctuation shows a sharp jump when the initial pressure decreases towards the limit both in the smooth tube and rough tube. Meanwhile, the transverse wave modes decrease from multi-head to single-head. Large velocity fluctuation and single-head spinning were observed when the limit occurs. In a rough tube, lower modes of the transverse wave were recorded at a fixed initial pressure as compared to a smooth tube. It is also found that as the detonation limits are approached, the longitudinal velocity fluctuation increases indicating an increase in instability and loss of robustness of the propagation detonation wave. The evolution of cell patterns follows closely to the velocity fluctuation trend. The detonation fails when it is devoid of cellular structure. Using this criterion, detonation limits are promoted in rough walled tubes although wall roughness may generate turbulent fluctuations to maintain a deflagration wave to propagate at a low-velocity regime. The ability of cellular instability growing is predominant in maintaining propagation of the self-sustained detonation. Lastly, this study focuses primarily on the increasing longitudinal velocity fluctuation of detonation wave fronts when limits are approached. To investigate further the high-speed deflagration wave supported by the turbulence fluctuations generated by the roughness, as well as different unsteady, unstable propagation modes of the wave propagation past the limits, e.g., galloping detonation, etc., a larger L/D test section is necessary to ensure the terminal wave behavior is attained.

Acknowledgment

This work is supported by the Natural Sciences & Engineering Research Council of Canada (NSERC). T. Ren is funded by the International Graduate Exchange Program of Beijing Institute of Technology.

References

1. Wolanski P. Detonative propulsion. Proc. Combust. Inst. 2013; 34: 125-158. https://doi.org/10.1016/j.proci.2012.10.005
2. Kailasanath K. Review of propulsion applications of detonation waves. AIAA J. 2000; 38: 1698–1708. https://doi.org/10.2514/2.1156
3. Roy GD, Frolov SM, Borisov AA, Netzer DW. Pulse detonation propulsion: challenges, current status, and future perspective. Prog. Energy Combust. Sci. 2004; 30: 545-672.

https://doi.org/10.1016/j.pecs.2004.05.001

4. Lee JHS. The Detonation Phenomenon. Cambridge University Press, Cambridge; 2008. https://doi.org/10.1017/CBO9780511754708
5. Camargo A, Ng HD, Chao J, Lee JHS. Propagation of near-limit gaseous detonations in small diameter tubes. Shock Waves 2010; 20(6): 499-508. https://doi.org/10.1007/s00193-010-0253-3
6. Gao Y, Ng HD, Lee JHS. Minimum tube diameters for steady propagation of gaseous detonations. Shock Waves 2014; 24(4): 447-454. https://doi.org/10.1007/s00193-014-0505-8
7. Zhang B, Pang L, Gao Y. Detonation limits in binary fuel blends of methane/hydrogen mixtures. Fuel 2016; 168: 27-33. https://doi.org/10.1016/j.fuel.2015.11.073
8. Zhang B, Liu H, Yan B. Investigation on the detonation propagation limit criterion for methane-oxygen mixtures in tubes with different scales. Fuel 2019; 239: 617-622. https://doi.org/10.1016/j.fuel.2018.11.062
9. Zhang B, Shen X, Pang L, Gao Y. Detonation velocity deficits of H2/O2/Ar mixture in round tube and annular channels. Int. J. Hydrogen Energy 2015; 40(43): 15078-15087. https://doi.org/10.1016/j.ijhydene.2015.09.036
10. Kitano S, Fukao M, Susa A, Tsuboi N, Hayashi AK, Koshi M. Spinning detonation and velocity deficit in small diameter tubes. Proc. Combust. Inst. 2009; 32(2): 2355-2362. https://doi.org/10.1016/j.proci.2008.06.119
11. Ishii K, Itoh K, Tsuboi T. A study on velocity deficits of detonation waves in narrow gaps. Proc. Combust. Inst. 2002; 29: 2789–2794. https://doi.org/10.1016/S1540-7489(02)80340-6
12. Ishii K, Monwar M. Detonation propagation with velocity deficits in narrow channels. Proc. Combust. Inst. 2011; 33(2): 2359-2366. https://doi.org/10.1016/j.proci.2010.07.051

13. Zhang B, Liu H, Yan B, Ng HD. Experimental study of detonation limits in methane-oxygen mixtures: Determining tube scale and initial pressure effects. Fuel 2020; 259, 116220. https://doi.org/10.1016/j.fuel.2019.116220
14. Wang LQ, Ma HH, Shen ZW, Yue B, Cheng YF, Fan ZQ. Experimental investigation of methane-oxygen detonation propagation in tubes. Appl. Thermal Eng. 2017; 123: 1300-1307. https://doi.org/10.1016/j.applthermaleng.2017.05.045
15. Zhang B, Chang XY, Bai CH. End-wall ignition of methane-air mixtures under the effects of CO_2/Ar/N_2 fluidic jets. Fuel 2020; 270, 117485. https://doi.org/10.1016/j.fuel.2020.117485
16. Dupré G, Joannon J, Knystautas R, Lee JHS. Unstable detonations in the near-limit regime in tubes. Symp. (Int.) Combust. 1991; 23: 1813-1820. https://doi.org/10.1016/S0082-0784(06)80461-3
17. Lee JJ, Dupré G, Knystautas R, Lee JH. Doppler interferometry study of unstable detonations. Shock Waves 1995; 5: 175-181. https://doi.org/10.1007/BF01435525
18. Haloua F, Brouillette M, Lienhart V, Dupré G. Characteristics of unstable detonations near extinction limits. Combust. Flame 2000; 122(4): 422-438. https://doi.org/10.1016/S0010-2180(00)00134-6
19. Lee JHS, Jesuthasan A, Ng HD. Near limit behavior of the detonation velocity. Proc. Combust. Inst. 2013; 34(2): 1957-1963. https://doi.org/10.1016/j.proci.2012.05.036
20. Zhang B, Liu H, Li Y. The effect of instability of detonation on the propagation modes near the limits in typical combustible mixtures. Fuel 2019; 253: 305-310. https://doi.org/10.1016/j.fuel.2019.05.006
21. Gao Y, Lee JHS, Ng HD. Velocity fluctuation near the detonation limits. Combust. Flame 2014; 161(11): 2982-2990. https://doi.org/10.1016/j.combustflame.2014.04.020

22. Gao Y, Ng HD, Lee JHS. Experimental characterization of galloping detonations in unstable mixtures. Combust. Flame 2015; 162: 2405-2413. https://doi.org/10.1016/j.combustflame.2015.02.007
23. Zhang B, Liu H, Yan BJ. Velocity behavior downstream of perforated plates with large blockage ratio for unstable and stable detonations. Aero. Sci. Tech. 2019; 86: 236-243. https://doi.org/10.1016/j.ast.2019.01.010
24. Zhang B， Liu H. The effects of large scale perturbation-generating obstacles on the propagation of detonation filled with methane–oxygen mixture. Combust. Flame 2017; 182: 279-287. https://doi.org/10.1016/j.combustflame.2017.04.025
25. Jackson S, Lee BJ, Shepherd JE. Detonation mode and frequency analysis under high loss conditions for stoichiometric propane-oxygen. Combust. Flame 2016; 167: 24-38. https://doi.org/10.1016/j.combustflame.2016.02.030
26. Zhang B, Wang C, Shen X, Yan L, Yan B, Xia Y. Velocity fluctuation analysis near detonation propagation limits for stoichiometric methane–hydrogen–oxygen mixture. Int. J. Hydrogen Energy 2016; 41: 17750-17759 https://doi.org/10.1016/j.ijhydene.2016.08.017
27. Cao W, Gao D, Ng HD, Lee JHS. Experimental investigation of near-limit gaseous detonations in small diameter spiral tubing. Proc. Combust. Inst. 2019; 37(3): 3555-3563. https://doi.org/10.1016/j.proci.2018.08.027
28. Wang LQ, Ma HH, Shen ZW, Pan J. Effects of bluff bodies on the propagation behaviors of gaseous detonation. Combust. Flame 2019; 201: 118-128. https://doi.org/10.1016/j.combustflame.2018.12.018
29. Wang LQ, Ma HH, Shen ZW, Chen DG. Experimental study of DDT in hydrogen-methane air mixtures in a tube filled with square orifice plates. Proc. Safety Environ. Protect. 2018; 116: 228-234. https://doi.org/10.1016/j.psep.2018.01.017

30. Wang LQ, Ma HH, Deng YX, Shen ZW. On the detonation behavior of methane-oxygen in a round tube filled with orifice plates. Proc. Safety Environ. Protect. 2019; 121: 263-270. https://doi.org/10.1016/j.psep.2018.11.002
31. Wang LQ, Ma HH, Shen ZW. Effect of orifice plates on detonation propagation in stoichiometric hydrogen-oxygen mixture. Exp. Thermal Fluid Sci. 2018; 99: 367-373. https://doi.org/10.1016/j.expthermflusci.2018.08.012
32. Cross M, Ciccarelli G. DDT and detonation propagation limits in an obstacle filled tube. J. Loss Prev. Process Ind. 2015; 36: 382-388. https://doi.org/10.1016/j.jlp.2014.11.020
33. Ciccarelli G, Cross M. On the propagation mechanism of a detonation wave in a round tube with orifice plates. Shock Waves 2016; 26(5): 587-597. https://doi.org/10.1007/s00193-016-0676-6
34. Ciccarelli G, Wang Z, Lu J, Cross M. Effect of orifice plate spacing on detonation propagation. J. Loss Prev. Process Ind. 2017; 49: 739-744. https://doi.org/10.1016/j.jlp.2017.03.014
35. Sun XX, Lu S. Effect of orifice plate on the transmission mechanism of a detonation wave in hydrogen-oxygen mixtures. Int. J. Hydrogen Energy 2020; 45(22): 12593-12603. https://doi.org/10.1016/j.ijhydene.2020.02.162
36. Teodorczyk A, Lee JHS, Knystautas R. Propagation mechanism of quasi-detonations. Proc. Combust. Inst. 1988; 22: 1723-1731. https://doi.org/10.1016/S0082-0784(89)80185-7
37. Zhang B. The influence of wall roughness on detonation limits in hydrogen–oxygen mixture. Combust. Flame 2016; 169: 333-339. https://doi.org/10.1016/j.combustflame.2016.05.003
38. Starr A, Lee JHS, Ng HD. Detonation limits in rough walled tubes. Proc. Combust. Inst. 2015; 35(2): 1989-1996. https://doi.org/10.1016/j.proci.2014.06.130

39. Zhang B, Liu H, Wang C. On the detonation propagation behavior in hydrogen-oxygen mixture under the effect of spiral obstacles. Int. J. Hydrogen Energy 2017; 42(33): 21392-21402. https://doi.org/10.1016/j.ijhydene.2017.06.201
40. Li J, Yang T, Wang X, Ning J. Propagation Mechanism of Detonations in Rough-Walled Tube. In: Int. Symp. on Shock Waves, pp. 253-260. Springer; 2017. https://doi.org/10.1007/978-3-319-91020-8_28
41. Teodorczyk A, Lee JHS. Detonation attenuation by foams and wire meshes lining the walls. Shock Waves 1995; 4: 225-236. https://doi.org/10.1007/BF01414988
42. Ren T, Yan Y, Zhao H, Lee JHS, Ng HD. Propagation of near-limit gaseous detonations in rough walled tubes. *Shock Waves* 2020; In press. https://doi.org/10.1007/s00193-020-00957-w
43. Liu Y, Lee JHS, Tan H, Ng HD. Investigation of near-limit detonation propagation in a tube with helical spiral. *Fuel* 2020; 286(2), 119384. https://doi.org/10.1016/j.fuel.2020.119384
44. Fay JA. Two-dimensional gaseous detonations: velocity deficit. Phys. Fluids 1959; 2: 283. https://doi.org/10.1063/1.1705924
45. Murray SB. Numa Manson on velocity deficits and detonation stability. Shock Waves 2008; 18: 255–268. https://doi.org/10.1007/s00193-008-0128-z
46. Zhang B, Liu H. Theoretical prediction model and experimental investigation of detonation limits in combustible gaseous mixtures. Fuel 2019; 258: 116-132. https://doi.org/10.1016/j.fuel.2019.116132
47. Crane J, Shi X, Singh AV, Tao Y, Wang H. Isolating the effect of induction length on detonation structure: hydrogen-oxygen detonation promoted by ozone. Combust. Flame 2019; 200: 44-52. https://doi.org/10.1016/j.combustflame.2018.11.008

48. Kee RJ, Rupley FM, Miller JA. Chemkin-II: A Fortran chemical kinetics package for the analysis of gas-phase chemical kinetics. Sandia national laboratories report SAND89-8009. USA: SAND89-8009, 1989.

49. Manson N, Brochet C, Brossard J, Pujol Y. Vibratory phenomena and instability of self-sustained detonations in gases. Proc. Combust. Inst. 1963; 9: 461-469. https://doi.org/10.1016/S0082-0784(63)80055-7

Declaration of interests

☒ The authors declare that they have no known competing financial interests or personal relationships that could have appeared to influence the work reported in this paper.

☐The authors declare the following financial interests/personal relationships which may be considered as potential competing interests:

Tianfei Ren: Conceptualization, Methodology, Visualization ,

Writing - Original Draft preparation,

Yiran Yan: Data curation, Investigation,

John H.S. Lee: Funding acquisition, Resources,

Hoi Dick Ng: Resources, Validation, Writing - Review &

Editing,

Qingming Zhang: Supervision,

Cheng Shang: Reviewing and Editing.